Research Article

Berberine Loaded Poly(vinylpyrrolidone) – Capped Silver Nanoparticles for Antioxidant and Antimicrobial Applications

B Dinesh[1], Lokesh Koodlur Sannegowda[2], Chandrashekhar G. Joshi[1]*

[1]Department of Biochemistry, Mangalore University, Mangalore - 574199, Karnataka, India.
[2]Department of Studies in Chemistry, Vijayanagara Sri Krishnadevaraya University, Ballari - 583 105, Karnataka, India.

(Received: 15-08-2025 Revised: 17-12-2025 Accepted: 24-12-2025)

Corresponding Author: ***Chandrashekhar G. Joshi*** Email: josheejoshee@gmail.com

ABSTRACT

Silver nanoparticles (AgNPs) are widely used in diverse fields, but have the limitation of stability and bioactivity which needs regular optimization. This study reports an ecofriendly approach in which the poly(vinylpyrrolidone) AgNPs was capped with glucose and loaded with Berberine(BBR) to form BBR loaded nanoformulation (PBR). The PBR was characterized using UV-visible spectroscopy, Scanning Electron Microscopy (SEM) with Energy Dispersive X-ray (EDX) analysis, X-ray diffraction, Dynamic Light Scattering (DLS), Zeta Potential analysis, and Fourier Transforms Infrared Spectroscopy (FTIR). The PBR showed a uniform spherical morphology with an average size of 78 nm and the zeta potential of -23.7 mV. FTIR study confirmed the loading of BBR through the shift in the functional groups in the spectra. PBR exhibited dose dependent antioxidant activity (18.5-45.9%), though lesser than the ascorbic acid. The antimicrobial activity revealed that PBR has moderate antifungal activity (40% inhibition against *Aspergillus* sp.). The moderate antioxidant and antifungal activity of PBR warrants further optimization to enhance its bioactivity.

Keywords: Silver nanoparticles; berberine; poly(vinylpyrrolidone); anti-oxidant activity; anti-microbial activity.

1. INTRODUCTION

The unique properties of the nanomaterials have revolutionized the advances in nanoscience and nanotechnology in the last decade [1]. Their size is 1-100 nm and these nanoparticles exhibit unique mechanical [2], electrical, magnetic, photochemical [3], and catalytic behaviors relative to those of their bulk counterparts [4]. The special features have helped them to have their applications in packaging, agriculture, energy, information technology, and health sectors [5].

AgNPs are notable metallic nanomaterials that have unique physical as well as chemical features [6]. They are extensively used in surface disinfectants, toys, textiles, air and water purification systems [7], gels, paints, food packaging, medical attire, and food product preservation [8]. Biological procedures of AgNPs synthesis have become popular because of the high cost and hazard posed by the conventional physical and chemical techniques [9, 10].

The AgNPs biological activity is controlled by various parameters, such as their shape, surface chemistry, size, coating, morphology, composition, ion release efficiency, agglomeration, dissolution rate, cell type and specific reducing agents [11]. Poly (vinylpyrrolidone) (PVP) is a widely applied as stabilizer and reducing agent in the AgNPs production because it establishes strong interaction with metals via its carboxyl group and the nitrogen atoms on its pyrrolidine ring [12]. Recent studies have highlighted the improved stability of AgNPs capped with PVP compared with other agents [13].

Berberine (BBR), is a plant derived isoquinoline alkaloid, traditionally used in Chinese medicine for treating range of conditions including microbial infections, diabetes mellitus, diarrhea, ulcers, hypercholesterolemia, cardiovascular issues, polycystic ovary syndrome, fatty liver, and cancer [14-16]. Even though BBR and P-AgNPs (PVP capped AgNPs) have been studied independently, the knowledge about BBR-loaded P-AgNPs remains limited.

This work was intended to prepare green P-AgNPs by use of PVP and glucose as capping and reducing agent respectively. We explored the improved stability of BBR due to PVP capping on AgNPs and evaluated the antioxidant and antimicrobial activity of BBR loaded P-AgNPs.

2. MATERIALS AND METHODS

Poly(vinylpyrrolidone) capped AgNPs Synthesis

Production of PVP-capped AgNPs followed the protocol of Chen *et al.*, [17]. To summarize, 15 mM $AgNO_3$ and PVP (1.5 mM in comparison with $AgNO_3$) dissolved in 50 mL of distilled water followed by stirring. Then, dropwise 10 mM glucose in 25 mL water and 10 mM KOH were added. The mixture was allowed to form the nanoparticles on a magnetic stirrer with heating plate at 60 degree temperature after this. The P-silver nanoparticles were then centrifuged at 11500 rpm (20 min) and collected after drying in stores.

P-AgNPs (PBR) loading of Berberine

The fusion of berberine (BBR) into P-AgNPs followed the protocol of Bhanumathi *et al.*, [18] with minor changes. In a short time, 10 mg P-AgNPs and 10 mg BBR were suspended in 5 mL dimethyl sulfoxide (DMSO) and stirred in each other overnight to allow binding. The resulting mixture was dialyzed against distilled water for 24 h to eliminate unbound components. Subsequently, centrifugation at 11,500 rpm was carried out to obtain the BBR-loaded P-AgNPs (PBR), separating them from free molecules and residual impurities.

UV– visible absorbance spectroscopy

PBR solution (0.5 ml) UV-1800 (Shimadzu, Japan) was investigated with precisions of ±1 nm at range of 200 to 700 nm wavelength and scan rate of 200 nm/min to confirm the formation of PBR through BBR loading on P-AgNPs. AgNO3 solution was used as a control at A (15 mM) [19].

Energy-dispersive X-ray spectroscopy and SEM

The morphology and dispersion of thin layers of PBR were studied using SEM applied on a copper grid plus carbon (ZEISS EVO 15, Germany). Elemental composition of the PBR was also determined by EDX (Oxford Instruments, AztecLive, UK) [20].

X-ray diffraction

X-ray diffractometer (Empyrean, 3 rd generation, Malvern PANalytical) 40 kV and 40 mA and Co K alpha radiation were utilized to find out the structural features of PBR. Peak broadening was the evidence of the crystalline structure of the nanoparticles. The DebyeScherrer equation was used to estimate the mean particle size [21] as follows.

$$D = \frac{K\lambda}{\beta Cos\theta} \quad (1)$$

D = depth of the nanocrystal,

K= constant,

λ= X Rays wavelength,

β = half maxima width at the (111) reflection at the angle of Bragg,

θ= Bragg's angle.

Zeta potential and dynamic light scattering

The laser diffraction with multiple scattering (3 LitesizerTM 500, Anton-Paar, Austria) was used to determine the hydrodynamic size of the PBR together with DLS. Zeta potential was found using a 3 LitesizerTM500(Anton-Paar, Austria) at 60 s and the mean zeta potential was found.

Fourier transform infrared spectroscopy

A Nicolet 6700 spectrometer operating with a resolution of 0.5 cm -1 were used to perform FTIR spectroscopy on both BBR and PBR using the KBr pellet technique. To do an analysis, the sample was finely ground with KBr, pressed into a transparent pellet, and loaded in the spectrometer holder. The spectra were measured within the 400 4000 cm -1 range, where the data on characteristic molecular vibrations and functional groups were obtained, and the structure of BBR and PBR [22] was characterized.

DPPH radical scavenging assay

The evaluation of this activity was done according to Hulikere *et al.*, [23] with slight modifications. PBR and ascorbic acid with different concentrations were added to 150 µL of DPPH solution (2 mM) and left to incubate after 15 min in the dark. A reading at 517 nm was then taken with an iMark microplate reader (Bio-Rad). The share of percentage of scavenging of free radical was calculated as follows:

$$Percentage\ of\ Radical\ Scavenging\ Activity = \left[\frac{Ac-As}{Ac}\right]\times 100 \qquad (2)$$

"Ac is the control absorbance of the DPPH radical + methanol;

As is the sample absorbance of the DPPH radical + sample AgNPs/Ascorbic acid"

Antimicrobial activity

PBR was tested against the pathogenic strains *Salmonella typhi*, *Escherichia coli*, *Staphylococcus aureus*, *Pseudomonas aeruginosa*, and fungus *Aspergillus sp*. through the well diffusion assay [24]. Agar plates were prepared by using 5 mm cork borer, and 100 µL of PBR at 100, 250, and 500 µg was loaded in the respective wells of 5 mm diameter of agar plates. Amikacin (25 µg/mL) and fluconazole (25 µg/mL) served to act as positive controls with bacterial and fungal strains, respectively.

Statistical analysis

Data from the experiments is presented in mean plus standard deviation (SD) of three independent repetitions. We conducted a statistical analysis with one-way ANOVA software Origin 8.0.

3. Results and Discussion

Evaluation of UV–visible spectroscopy

PBR UV-visible spectral analysis was done to ensure that the BBR has been loaded successfully on the surface of the P-AgNPs (Figure 1). Characteristic absorption peaks of BBR were observed at 232, 266, 346, and 428 nm, consistent with findings of Daiz *et al.*, [25]. Upon interaction with P-AgNPs, peaks were shifted toward 220, 260, 348, and 425 nm indicating the formation of PBR [18].

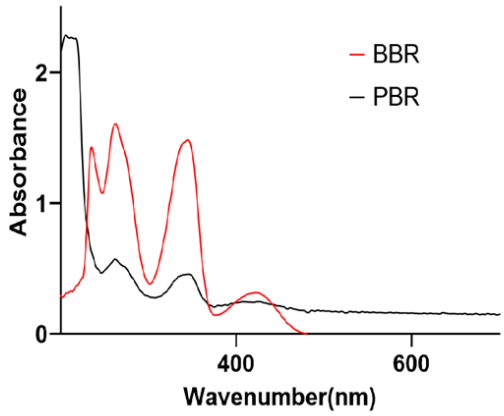

Figure 1: Ultraviolet-visible absorption spectra of Berberine (BBR) and P-AgNPs loaded with BBR (PBR)

Energy dispersive X-ray spectroscopy and SEM

SEM imaging was employed to examine the surface of PBR (Figure 2a). The images revealed the uniformly distributed, spherical, non-aggregated particles ranging from 60–100 nm in diameter with a mean particle size of 78 nm. In comparison, Bhanumathi et al have reported the size range of 35–50 nm for BBR-loaded AgNPs based on transmission electron microscopic studies [18]. The differences in the results are due to the use of different electron microscopes which work on dissimilar principles yielding slight variation in morphological data.

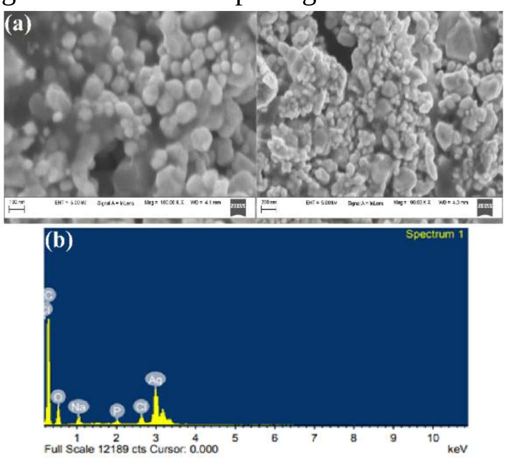

Figure 2: The morphology and elemental composition of P-AgNPs loaded with Berberine (PBR) in (a) SEM and (b) EDX

The energy dispersive X-ray (EDX) analysis with at 3 KeV absorption peak, revealed the purity and complete chemical composition of the PBR (Figure 2b). A significant peak was observed for silver (12.45%) along with other notable components such as oxygen (52%), sodium (4.4%), chlorine (2.36%), and carbon (26.9%). Our results establish the role of the other organic molecules in the capping and stabilization of PBR [26].

X-ray diffraction evaluation

XRD pattern revealed clear diffraction peaks at 38.07 °, 44.32 °, 64.42 °, 77.35 °, and 81.45 ° as the crystal structure of the fcc metallic silver crystallographic plane (111), (200), (220), (311), and (222) (Figure 3). The lattice constant (4.047), interplanar spacing values (dhl) of 2.363, 2.043, 1.446, 1.232, and 1.180 were also matching with the standard Ag values JCPDS-PDF -card 04-0783. Weak signals at 10.0 ° and 20.0 ° are explained by BBR [27].

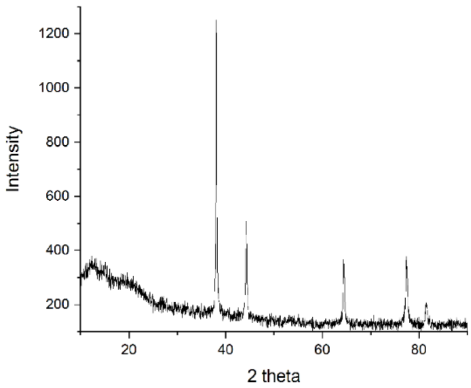

Figure 3: X-ray diffraction pattern of P-AgNP loaded with Berberine (PBR)

Evaluation of Zeta Potential and Dynamic light scattering

DLS evaluation using light interaction of PBR revealed the average hydrodynamic diameter of 284 nm (96% intensity) as shown in Figure 4a. The bigger size of the PBR observed in DLS compared to XRD, and SEM is attributed to the impact of the coating, stabilizing materials that build up on the surface, and the metallic core [28]. In addition, non-uniform dispersion of particles in the colloidal solution used in the DLS is also responsible for the observed differences in the results.

The surface charge of PBR and its stability were assessed by Zeta potential analysis (Figure 4b). PBR exhibited a modest stability with 23.7 mV zeta potential. Even though the PBR did not displayed the strong positive or negative zeta potential (greater than ±30 mV) required for particle separation and disaggregation [29], negative charge resist the aggregation and promote the stability due to electrostatic repulsion.

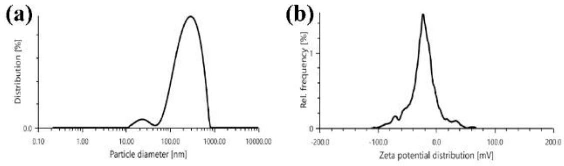

Figure 4: a) Hydrodynamic size measured by DLS, b) Surface charge determined by zeta potential analysis of P-AgNP loaded with BBR (PBR)

Fourier transform infrared Spectroscopic evaluation

The FTIR of PBR (Figure 5) spectrum was characterized by clear absorption bands at 1000.44, 1634.52, 2847.53, 2964.84 and 3548.85 cm $^{-1}$. The band of 1634.52 cm^{-1} OH is associated with the carbonyl (C=C) of BBR, which proves that it becomes conjugated with P-AgNPs. The peaks at 2847.53 cm^{-1} and 2964.84 cm^{-1} of the aliphatic C–H stretching vibrations are due to either PVP or BBR attached to the nanoparticles. The strong band at 3548.85 cm^{-1} showed the presence –OH or –NH group in the compound. All in all, the FTIR results show that BBR is conjugated to P-AgNPs

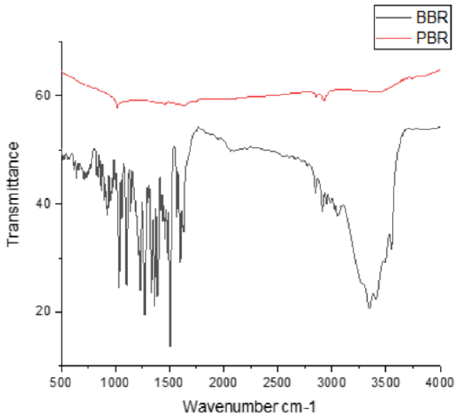

Figure 5: the FTIR spectra of berberine (BBR) and of P-AgNP loaded with BBR (PBR).

DPPH radical scavenging assay

This assay was employed to determine PBR antioxidant activity at 0.4-2mg/mL (Figure 6). PBR increased its radical scavenging activity in dose-dependent manners, reaching a maximum DPPH scavenging activity of 45.9% at the highest concentration tested. Even though its activity was relatively lower than the standard ascorbic acid, an apparent improvement in the activity with higher concentration was noted. It is possible that the antioxidant activity of PBR remains observed due to the functional groups of BBR conjugated with P-AgNPs.

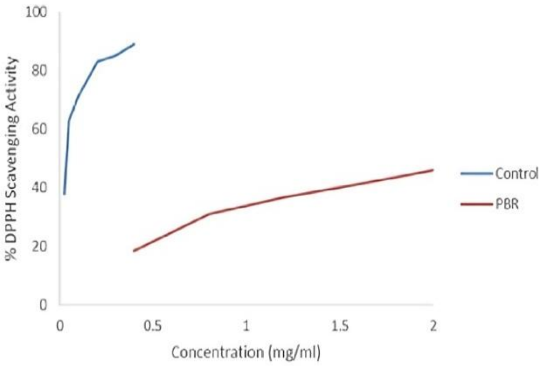

Figure 6: DPPH radical scavenging activity (%) of Control and PBR at different concentrations (mg/mL)

Antimicrobial activity

PBR and amikacin were tested against the microbe *E. coli, P. aeruginosa, S. aureus, and S. typhi*. The tested bacteria did not show any antibacterial action in the PBR. The non-toxic PVP capping to AgNPs, the particle size, and the special ways of action explain the lack of the antibacterial action [30, 31]. In comparison, PBR displayed 40% of the standard drug inhibition of *Aspergillus sp.* growth. Although the fungal growth inhibition power of PBR was lesser than fluconazole (Table 1 & Figure 7), results indicate the potential antifungal activity of PBR, warranting further optimization.

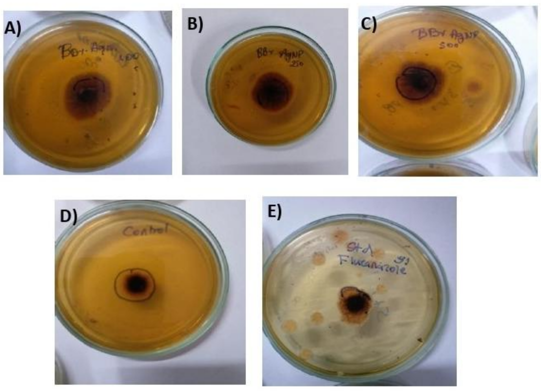

Figure 7: Antifungal activity of PBR against Aspergillus sp. showing zones of inhibition at different concentrations: (A) 100 µg, (B) 250 µg, (C) 500 µg of PBR. (D) Control, and (E) standard (fluconazole).

Table 1: Anti-microbial activity of the P-AgNP loaded with BBR (PBR), and standard (Amikacin and Fluconazole).

Test organism	PBR	Amikacin	Fluconazole	Control
	Zone of inhibition (mm)			
S.typhi	-	12±0.6	-	-
P.auriginosa	-	11±0.3	-	-
E.coli	-	10±0.7	-	-
S.aureus	-	9±0.4	-	-
Aspergillus sp.	3±0.4	-	2±0.7	-

4. Conclusion

In this study, AgNPs were synthesized, capped with PVP and loaded with BBR employing glucose as reducing agent at 60 °C under alkaline conditions without using any harsh chemicals. P-AgNPs and PBR formation was validated by using UV-visible spectroscopy, and their crystalline nature was established through XRD analysis. The SEM and EDX analyses revealed that their size was approximately 78 nm and was composed primarily of carbon, silver, and sodium. The zeta potential and the hydrodynamic size were -23 mV and 284 nm, respectively. The analysis of FTIR showed the successful loading of BBR onto P-silver nanoparticles. The PBR composite exhibited significant radical scavenging activity, moderately active against *Aspergillus* sp. and did not exhibit any antibacterial activity likely due to its size and morphology. These studies confirm the biomedical applications of the PBR warranting further studies to enhance the therapeutic efficacy.

Acknowledgement

The authors gratefully acknowledge DST-PURSE, Mangalore University, and NITK-Surathkal for providing facilities and support in sample analysis.

Author Contributions

Dinesh B was involved in the investigation, analysis of data, collection of data, writing of original draft, reviewing as well as editing, administration of the project and funding acquisition. Lokesh Koodlur Sannegowda helped to write the manuscripts, FTIR interpretation of data, and editing and reviewing. Chandrashekhar G. Joshi took part in the creation of the work, and designing methods of investigation, validation, formal analysis, data curation, provision of resources, reviewing and editing of the manuscript, and overseeing the work.

Declaration
Ethical approval was not applicable.

Funding
Funding is not applicable.

Conflicts of interest
The author's do not have any conflicts of interest.

REFERENCES:
1. Bayda S, Adeel M, Tuccinardi T, Cordani M, Rizzolio F. The History of Nanoscience and Nanotechnology: From Chemical-Physical Applications to Nanomedicine. *Molecules*. 2019 Dec 27;25(1):112.
2. Baig N, Kammakakam I, Falath W. Nanomaterials: a review of synthesis methods, properties, recent progress, and challenges. 2021 Mar 29 [cited 2025 July 14]; Available from: https://pubs.rsc.org/en/content/articlehtml/2021/ma/d0ma00807a
3. Wahab HU, Eisa MH, Binzowaimil AM, Narasimharao K, Suleiman SM, Khan M. Investigation of the photocatalytic potential of silver nanoparticles for the photodegradation of neutral red chloride dye in aqueous medium through experimental and DFT study. *Journal of Molecular Structure* [Internet]. 2026 Jan 15 [cited 2025 Dec 17];1350:144126. Available from: https://www.sciencedirect.com/science/article/pii/S0022286025027723
4. Aththanayaka S, Thiripuranathar G, Ekanayake S. Emerging advances in biomimetic synthesis of nanocomposites and potential applications. Materials Today Sustainability [Internet]. 2022 Dec 1 [cited 2025 July 14];20:100206. Available from: https://www.sciencedirect.com/science/article/pii/S2589234722000987
5. Calderón-Jiménez B, Johnson ME, Montoro Bustos AR, Murphy KE, Winchester MR, Vega Baudrit JR. Silver Nanoparticles: Technological Advances, Societal Impacts, and Metrological Challenges. *Front Chem*. 2017;5:6.
6. Goel M, Sharma A, Sharma B. Recent Advances in Biogenic Silver Nanoparticles for Their Biomedical Applications. *Sustainable Chemistry* [Internet]. 2023 Mar [cited 2025 July 14];4(1):61–94. Available from: https://www.mdpi.com/2673-4079/4/1/7
7. Vishwanath R, Negi B. Conventional and green methods of synthesis of silver nanoparticles and their antimicrobial properties. *Current Research in Green and Sustainable Chemistry* [Internet]. 2021 Jan 1 [cited 2025 July 14];4:100205. Available from: https://www.sciencedirect.com/science/article/pii/S2666086521001521
8. Bruna T, Maldonado-Bravo F, Jara P, Caro N. Silver Nanoparticles and Their Antibacterial Applications. *International Journal of Molecular Sciences* [Internet]. 2021 Jan [cited 2025 July 14];22(13):7202. Available from: https://www.mdpi.com/1422-0067/22/13/7202
9. Zhang XF, Liu ZG, Shen W, Gurunathan S. Silver Nanoparticles: Synthesis, Characterization, Properties, Applications, and Therapeutic Approaches. *Int J Mol Sci*. 2016 Sept 13;17(9):1534.
10. Bhardwaj B, Singh P, Kumar A, Kumar S, Budhwar V. Eco-Friendly Greener Synthesis of Nanoparticles. *Adv Pharm Bull* [Internet]. 2020 Sept [cited 2025 July 14];10(4):566–76. Available from: https://www.ncbi.nlm.nih.gov/pmc/articles/PMC7539319/
11. Xu L, Wang YY, Huang J, Chen CY, Wang ZX, Xie H. Silver nanoparticles: Synthesis, medical applications and biosafety. *Theranostics*. 2020;10(20):8996–9031.
12. Koczkur KM, Mourdikoudis S, Polavarapu L, Skrabalak SE. Polyvinylpyrrolidone (PVP) in nanoparticle synthesis. *Dalton Trans* [Internet]. 2015 Oct 13 [cited 2025 July 14];44(41):17883–905. Available from: https://pubs.rsc.org/en/content/articlelanding/2015/dt/c5dt02964c

13. Safo IA, Werheid M, Dosche C, Oezaslan M. The role of polyvinylpyrrolidone (PVP) as a capping and structure-directing agent in the formation of Pt nanocubes. *Nanoscale Adv* [Internet]. 2019 Aug 6 [cited 2025 July 14];1(8):3095–106. Available from: https://pubs.rsc.org/en/content/articlelanding/2019/na/c9na00186g
14. Javed Iqbal M, Quispe C, Javed Z, Sadia H, Qadri QR, Raza S, *et al.,* Nanotechnology-Based Strategies for Berberine Delivery System in Cancer Treatment: Pulling Strings to Keep Berberine in Power. *Front Mol Biosci* [Internet]. 2021 Jan 15 [cited 2025 July 14];7. Available from: https://www.frontiersin.org/journals/molecular-biosciences/articles/10.3389/fmolb.2020.624494/full
15. Nadalin P, Kim YG, Park SU. Recent studies on berberine and its biological and pharmacological activities. *EXCLI J* [Internet]. 2023 Feb 28 [cited 2025 July 14];22:315–28. Available from: https://www.ncbi.nlm.nih.gov/pmc/articles/PMC10201012/
16. Zhu C, Li K, Peng XX, Yao TJ, Wang ZY, Hu P, *et al.,* Berberine a traditional Chinese drug repurposing: Its actions in inflammation-associated ulcerative colitis and cancer therapy. *Front Immunol* [Internet]. 2022 Dec 6 [cited 2025 July 14];13. Available from: https://www.frontiersin.org/journals/immunology/articles/10.3389/fimmu.2022.1083788/full
17. Chen Q, Liu G, Chen G, Mi T, Tai J. Green Synthesis of Silver Nanoparticles with Glucose for Conductivity Enhancement of Conductive Ink. *BioResources* [Internet]. 2016 Nov 29 [cited 2025 Sept 13];12(1):608–21. Available from: https://bioresources.cnr.ncsu.edu/resources/green-synthesis-of-silver-nanoparticles-with-glucose-for-conductivity-enhancement-of-conductive-ink/
18. Bhanumathi R, Vimala K, Shanthi K, Thangaraj R, Kannan S. Bioformulation of silver nanoparticles as berberine carrier cum anticancer agent against breast cancer. *New J Chem* [Internet]. 2017 Nov 20 [cited 2025 July 14];41(23):14466–77. Available from: https://pubs.rsc.org/en/content/articlelanding/2017/nj/c7nj02531a
19. Ashraf JM, Ansari MA, Khan HM, Alzohairy MA, Choi I. Green synthesis of silver nanoparticles and characterization of their inhibitory effects on AGEs formation using biophysical techniques. *Sci Rep.* 2016 Feb 2;6:20414.
20. Dinesh B, Monisha N, Shalini HR, Prathap GK, Poyya J, Shantaram M, *et al.,* Antibacterial activity of silver nanoparticles synthesized using endophytic fungus-*Penicillium cinnamopurpureum*. *Spectroscopy Letters* [Internet]. 2022 Jan 2 [cited 2025 July 14];55(1):20–34. Available from:https://doi.org/10.1080/00387010.2021. 201 0764
21. Danagoudar A, Pratap GK, Shantaram M, Ghosh K, Kanade SR, Joshi CG. Characterization, cytotoxic and antioxidant potential of silver nanoparticles biosynthesised using endophytic fungus (*Penicillium citrinum* CGJ-C1). *Materials Today Communications* [Internet]. 2020 Dec 1 [cited 2025 Sept 13];25:101385. Available from:https://www.sciencedirect.com/science/ article/pii/S2352492820323965
22. Dinesh B, Chethan MU, Pratap GK, Poyya J, Shantaram M, Hampapura JS, *et al.,* Biogenic Synthesis of Silver Nanoparticles using Aspergillus Aureoles (Endophyte) and Demonstration of their Antimicrobial Activity. *Analytical Chemistry Letters* [Internet]. 2021 Nov 2 [cited 2025 July 14];11(6):899–910. Available from: https://doi.org/10.1080/22297928.2021.2007789
23. Manjunath Hulikere M, Joshi CG. Characterization, antioxidant and antimicrobial activity of silver nanoparticles synthesized using marine endophytic fungus-*Cladosporium cladosporioides*. *Process Biochemistry* [Internet]. 2019 July 1 [cited 2025 Sept 13];82:199–204. Available from: https://www.sciencedirect.com/science/article/pii/S1359511318316994

24. Chougale R, Kasai D, Nayak S, Masti S, Nasalapure A, Raghu AV. Design of eco-friendly PVA/TiO2-based nanocomposites and their antifungal activity study. *Green Materials* [Internet]. 2020 Mar [cited 2025 July 14];8(1):40–8. Available from: https://www.icevirtuallibrary.com/doi/abs/10.1680/jgrma.19.00002
25. Díaz MS, Freile ML, Gutiérrez MI. Solvent effect on the UV/Vis absorption and fluorescence spectroscopic properties of berberine. *Photochem Photobiol Sci* [Internet]. 2009 July 1 [cited 2025 July 14];8(7):970–4. Available from: https://pubs.rsc.org/en/content/articlelanding/2009/pp/b822363g
26. Nedumaran N, Suresh N, Gurumoorthy K. Fabrication of Polydopamine with Silver Nanoparticles Coating on Titanium to Enhance Corrosion Resistance: An *In-vitro* Analysis. J*ournal of Pioneering Medical Sciences* [Internet]. 2025 July 5 [cited 2025 Dec 17];14:138-45. Available from: https://jpmsonline.com/article/fabrication-of-polydopamine-with-silver-nanoparticles-coating-on-titanium-to-enhance-corrosion-resistance-an-i*n-vitro*-analysis-767/
27. Bhanumathi R, Manivannan M, Thangaraj R, Kannan S. Drug-Carrying Capacity and Anticancer Effect of the Folic Acid- and Berberine-Loaded Silver Nanomaterial To Regulate the AKT-ERK Pathway in Breast Cancer. *ACS Omega* [Internet]. 2018 July 31 [cited 2025 July 14];3(7):8317–28. Available from: https://doi.org/10.1021/acsomega.7b01347
28. Mourdikoudis S, Pallares RM, Thanh NTK. Characterization techniques for nanoparticles: comparison and complementarity upon studying nanoparticle properties. *Nanoscale* [Internet]. 2018 July 13 [cited 2025 July 14];10(27):12871–934. Availablefrom:https://pubs.rsc.org/en/content/articlelanding/ 2018/nr/c8nr02278j
29. Németh Z, Csóka I, Semnani Jazani R, Sipos B, Haspel H, Kozma G, *et al.*, Quality by Design-Driven Zeta Potential Optimisation Study of Liposomes with Charge Imparting Membrane Additives. *Pharmaceutics.* 2022 Aug 26;14(9):1798.
30. Ferdous Z, Nemmar A. Health Impact of Silver Nanoparticles: A Review of the Biodistribution and Toxicity Following Various Routes of Exposure. *Int J Mol Sci.* 2020 Mar 30;21(7):2375.
31. Elmehalawy NG, Zaky MMM, Eid AM, Fouda A. Eco-friendly synthesis of silver nanoparticles: multifaceted antioxidant, antidiabetic, anticancer, and antimicrobial activities. *Sci Rep* [Internet]. 2025 Oct 27 [cited 2025 Dec 17];15(1):37349. Available from:https://www.nature.com/articles/s41598-025-22154-4